

1D Models for Enzymatic Biological Fuel Cells

by Scott Calabrese Barton

Enzyme electrocatalysts offer an intriguing approach to the design of fuel cell systems by broadening the range of fuel and oxidants available and by introducing potentially low cost organic and transition metal catalysts that are literally highly evolved.¹ Increased understanding of redox enzymes will further our ability to design catalyst active sites and possibly lead to breakthroughs in electrocatalytic technology.

Enzymes are proteins that catalyze chemical reactions. Oxidoreductase enzymes specifically catalyze oxidation-reduction reactions.² These enzymes can be implemented in biological fuel cells to convert chemical energy from fuels such as glucose, ethanol, or hydrogen to electrical energy. One enzyme, such as glucose oxidase, might oxidize a sugar molecule such as glucose to produce electrons and protons at an anode.³ The free electron might then flow through an external circuit to a cathode, thereby producing electrical current. At the cathode, the electron can be used to reduce oxygen, a reaction that can be catalyzed by an additional enzyme such as laccase.⁴ The reduced oxygen can combine with the proton to form water, completing the electrical circuit.

The design and analysis of bioelectrocatalytic systems, not only for fuel cells but also for biosensor and bioconversion applications, requires detailed quantitative understanding of the physicochemical phenomena controlling such systems. A qualitative understanding alone can only go so far in terms of predicting performance, and is a very weak approach to teasing apart the thermodynamic, kinetic, and transport phenomena that can potentially control reaction rates. For example, one may wish to compare the kinetic aspects of two enzymes in an electrochemical system in which significant mass transport limitations are present. It may be possible in some rare circumstances to eliminate the mass transport control by manipulation of the experiment. But in most cases, such mass transport limitations can only be minimized, and quantified in terms of rigorous models. To get at the kinetics aspects, an analysis is performed to estimate and subtract off the driving force that is devoted to transport, such that the relation between driving force and kinetic rate

can be estimated. This process requires not only a model for transport in the system, but also a model for the kinetics, in terms of the relationship between driving force and the kinetically-controlled rate.

Similarly, the desire to build real-world systems with bioelectrocatalysts requires engineering approaches to predict real-world performance, including the effect of length scales on device efficiency or temperature due to increased limitations of heat and mass transport at large length scales. Temperature effects may be particularly important for enzymatic systems, where the activity and durability of the biocatalysts is usually maximized within a very tight temperature range.

This article describes some simple modeling approaches for enzymatic fuel cells that are applicable to many other systems, including biosensors and bioreactors. These topics are taken from a broad swath of literature, with some emphasis on recent advances. We discuss basic thin film 1D models and their analytical and numerical solutions, and then introduce the treatment of porous bioelectrodes, which covers the vast majority of practical devices. Finally we describe one type of complete cell model.

Simplifying assumptions ▶ Any approach to analyzing a system as complex as an enzymatic electrode requires simplification. We begin by addressing only one-dimensional, constant-temperature, steady state systems. Proton transport has a significant impact on enzyme kinetics, but we will roll that dependence into the kinetics by treating all rate constants as pH dependent. We will also ignore potential fields and the resulting migration losses, by assuming the low current densities associated with enzyme reactions. Similarly, convection will be ignored within the electrode in favor of diffusion, and thermodynamic partitioning of species into various phases will similarly be ignored.

Electron transport ▶ Two basic mechanisms for enzyme electrocatalysis are considered in the literature: Direct Electron Transfer (DET) and Mediated Electron Transfer (MET).⁵ In DET, the enzyme is immobilized directly on an electrode surface, presumably with the active center of the enzyme within 1 nm or so of the electrode surface.

(continued on next page)

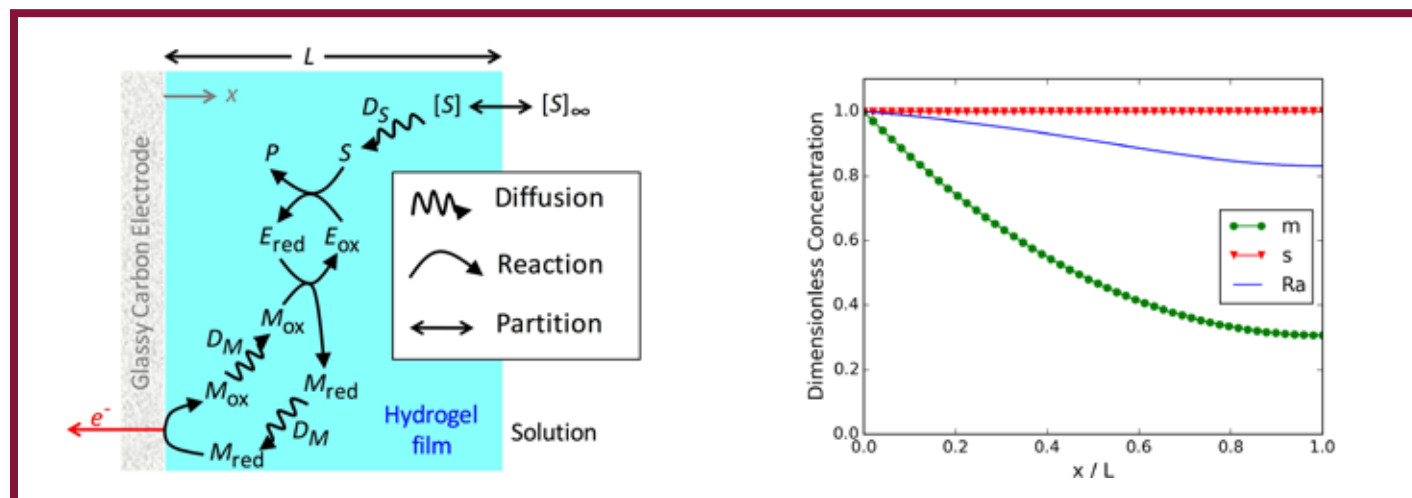


FIG. 1. 1D mediated bioelectrode model. (a) Schematic of a 1D model of a mediated glucose-oxidizing electrode, modified from Ref. 2. (b) Normalized concentration profiles for mediator, m , substrate s , and normalized reaction rate, Ra . For this case, the substrate concentration is uniform, and mass transfer limitations exist only for the mediator. The reaction rate varies nonlinearly with mediator concentration.

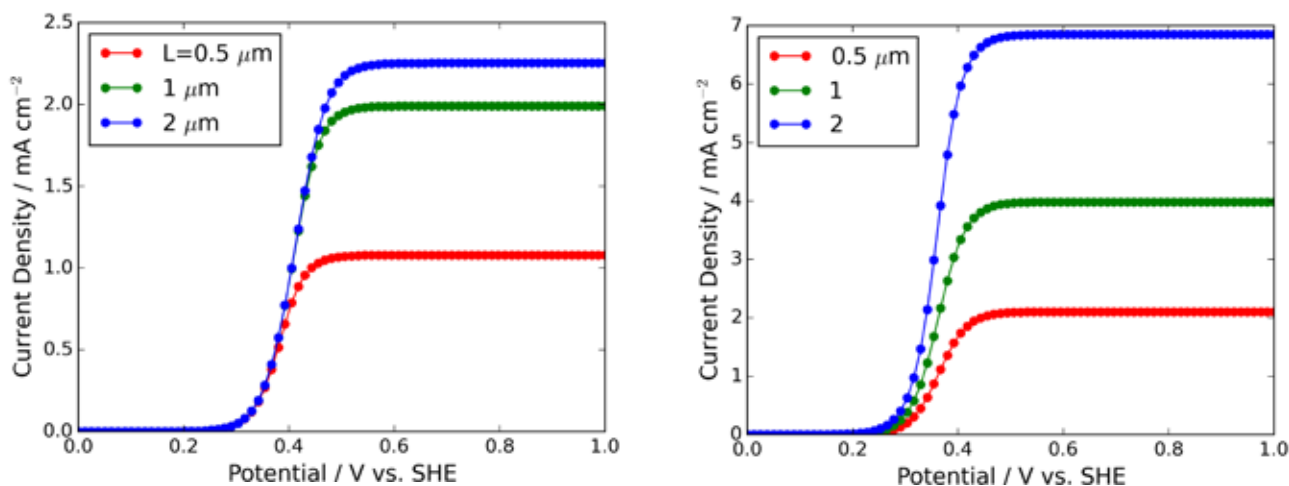


Fig. 2. Numerically calculated polarization of a 1D bioelectrode at various film thicknesses, L . (a) Planar film showing reduced utilization as loading increases. (b) Porous electrode showing improved, but not perfect, utilization.

Under these conditions, electrons are able to tunnel directly from the solid electrode phase into the enzyme, and vice versa. Combined with electron transfer to the substrate, this electron transfer current density therefore obeys a Butler-Volmer like dependence on potential:

$$i = i_0 \{ \exp((V - U) / b) - \exp(-(V - U) / b) \} \quad (1)$$

Here, i is current density, i_0 the exchange current density, V the electrode potential, U is reversible potential (where $i = 0$) and b is the Tafel slope.

Thin Film Model

In contrast, MET involves an additional molecular species, the mediator, that shuttles electrons between the electrode surface and an enzyme site that might be multiple microns away. This introduces issues of electron transfer between the electrode and mediator, transport of electrons by the mediator, and electron transfer between the mediator and the enzyme, shown schematically in Fig. 1a. Ideally, these processes occur with a thin film (the blue region of thickness L in Fig. 1a) where the enzyme and mediator are entrapped.

Surface-mediator electron transfer can be thought to follow Butler-Volmer kinetics, similar to DET. These kinetics are typically sufficiently fast to assume that the reactions are in equilibrium. In this case one can assume that the reduced and oxidized mediator concentrations (M_{ox} and M_{red} respectively) exist at the electrode surface in a ratio related to the electrode potential, V and redox potential of the mediator, U , by the Nernst Equation:

$$V = U + \frac{nF}{RT} \log \frac{M_{\text{ox}}}{M_{\text{red}}} = U + \frac{nF}{RT} \log \frac{M_{\text{ox}}}{M_{\text{tot}} - M_{\text{ox}}} \quad (2)$$

where F is Faraday's constant, R is the gas constant, T is temperature, and n is the number of electrons transferred between M_{ox} and M_{red} (typically $n = 1$). Here we have used the fact that the total mediator concentration, M_{tot} , is the sum of M_{ox} and M_{red} .

Transport of reactants occurs primarily by diffusion in electrolyte of sufficient ionic conductivity. The Nernst equation therefore describes the one-dimensional flux, N , of all species:

$$N_M = -D_M \frac{dM}{dx} ; N_S = -D_S \frac{dS}{dx} \quad (3)$$

Here, D_M and D_S represent the diffusivity of mediator and substrate, respectively, M and S are concentration, and x is spatial position. The

species in question are typically the mediator and substrate (Fig. 1a) but the concept of diffusivity is complicated when applied to the mediator. The mediator may be either a freely diffusing molecule, such as quinone, or an immobilized redox complex such as a redox polymer. For a redox polymer, the diffusivity D_i refers to the apparent diffusion of electrons through the polymer, because the redox moieties themselves do not move.⁶ Additionally, if conductivity is low, migration effects due to potential gradients must be considered.⁷

Kinetics at the enzyme involve the simultaneous oxidation of mediator combined with reduction of the oxidant (at a cathode) or mediator reduction/fuel oxidation (anode). The kinetics can be quite complex, involving reactant-enzyme binding, reversibility, inhibition, and cooperativity in multi-site enzymes. Full-blown kinetics may include some dozens of parameters, and simplifications are usually required. For example, if only one form of the mediator exists in significant quantity, irreversible kinetics may be assumed. The simplest enzyme rate expression that accounts for mediator and substrate binding is the ping-pong expression:⁸

$$r = \frac{k_{\text{cat}} EMS}{K_M S + K_S M + MS} \quad (4)$$

where k_{cat} , K_M , and K_S are rate constants. This expression is not applicable to all enzymes, however, and more generalized approaches that account for reversibility and other kinetic mechanisms are available. Examples include the Hanekom and Liebermaster generalized rate laws.⁹

In 1D at steady-state and neglecting migration, the rate of change of diffusive flux of both mediator and substrate is related directly to the enzymatic reaction, leading to two second-order differential equations:¹⁰⁻¹²

$$-\frac{dN_M}{dx} = D_M \frac{d^2 M}{dx^2} = \frac{v_S k_{\text{cat}} EMS}{K_M S + K_S M + MS} \quad (5)$$

$$-\frac{dN_S}{dx} = D_S \frac{d^2 S}{dx^2} = \frac{v_S k_{\text{cat}} EMS}{K_M S + K_S M + MS} \quad (6)$$

Boundary conditions depend strongly on the physical system of interest. For example, the solid electrode is impermeable to the substrate, so the flux of substrate, N_S , is zero there. Similarly, the mediator may be retained in the electrode film, so the flux of mediator at the electrolyte film, N_M , is zero. Lastly, the Nernst equation (Eq. 2) can be used to relate the mediator concentration at the electrode to the

potential, and the bulk concentration at the electrolyte interface may be assumed. To summarize the boundary conditions:

$$\begin{aligned} \text{at } x = 0 : V = U + \frac{nF}{RT} \log \frac{M_{ox}}{M_{tot} = M_{ox}} ; \frac{dS}{dx} = 0 \\ \text{at } x = L : \frac{dM}{dx} = 0 ; S = S_0 \end{aligned} \quad (7)$$

The above equations represent a nonlinear set of coupled differential equations, whose solution can only be found numerically. Numerical solutions abound in the literature.¹⁰⁻¹² If simplifying assumptions are made, however, analytical solutions may be found. Bartlett et al. explore analytical solutions for simplified cases of these equations in detail.¹⁰ More recently, Rajendran has reported an analytical solution for the case where the electrode is saturated in substrate, $S \gg K_S$.¹³ Figure 1b shows a plot of mediator and substrate concentrations as well as the enzyme reaction rate as a function of position, calculated numerically for some typical conditions. Python code for this numerical solution is available online.¹⁴

Because this is an electrode, we are primarily interested in the current generated. We can calculate the current density as from the mediator flux at the electrode surface according to Fick's law:

$$i = -nFD \left. \frac{dM}{dx} \right|_{x=0} \quad (8)$$

Figure 2a shows a polarization plot of current density vs. electrode potential for a range of electrode thicknesses, L . We see that the plateau current approximately doubles from $L = 0.5$ to $1 \mu\text{m}$, but increases only a small amount at $L = 2 \mu\text{m}$, due to mediator mass transport limitations that lead to reduced enzyme utilization.

Porous Electrode Model

Practical electrodes require high surface area to achieve relevant current densities. In the case of biological fuel cells, this is most often achieved by immobilizing a thin film of the enzyme catalyst (plus mediator) on the surface of a high-surface area solid conductor such as carbon. There is some risk of immobilizing the enzyme directly on the carbon surface due to the possibility of denaturation.¹⁵ In the case of hydrogel bioelectrodes, the risk is mitigated by the stabilization effect of the hydrogel as well as the reduced amount of enzyme directly contacting the surface.

Using a macrohomogeneous approach, the above thin film model can be applied to a porous electrode. The main new parameters to be introduced are the conductor surface area per volume, a , the porosity, ϵ , and the porous electrode thickness L_p . The thin film model is used to calculate the local consumption rate, R_p , within the porous structure, assuming some effective film thickness. For example, assuming

a roughness factor aL_p , the film thickness of the porous electrode would be $L/(aL_p)$ where L is the film thickness for the planar case. The resulting material balance on the substrate becomes:

$$-\frac{dN_s}{dy} = D_s^e \frac{d^2M}{dy^2} = aR_p S \quad (9)$$

where D_s^e is the effective diffusivity of substrate in the porous electrode, and y is the position within the porous electrode. Here we continue to neglect migration and convection terms. Using similar boundary conditions as the thin film model,

$$\text{at } y = 0 : \frac{dS}{dy} = 0 ; \text{ at } y = L_p : S = S_0 \quad (10)$$

We may solve this system numerically for the substrate concentration profile within the electrode, and calculate the current density as it relates to the substrate gradient concentration at the electrode-electrolyte interface

$$i = nFD_s^e \left. \frac{dS}{dy} \right|_{L_p} \quad (11)$$

As an example, Fig. 2b shows polarization curves for a glucose-oxidizing electrode using Toray paper as a substrate, for varying loading, L . Here the surface roughness was calculated by electrochemical capacitance measurements.¹⁶ Utilization of the enzyme is improved, as the plateau current is approximately linearly dependent on L . However, the plateau does not reach the expected 8 mA cm^{-2} for $L = 2 \mu\text{m}$ because substrate transport becomes rate limiting. Python code for this numerical solution is also provided online.¹⁴ We have previously extended this approach to gas diffusion electrodes.¹⁷

Complete Cell Model

The above approaches can be combined to obtain a complete cell model. In this case, one typically wishes to prepare two electrode models that have matching current density, coupled via a common electrolyte. This common electrolyte might also contain substrates for each electrode- for example glucose for the anode and oxygen for the cathode. It is important to consider the effect of the each reactant at each electrode- for example oxygen is a natural substrate of glucose oxidase but glucose does not affect the activity of laccase at a laccase-catalyzed oxygen electrode.

To match current densities, one may choose to change the boundary conditions in Eq. 7, or just iterate the model over a range of potentials until the current densities at each electrode match a desired value. The latter approach is shown in Fig. 3, where the polarization of individual laccase and glucose oxidase electrodes are shown alongside the overall cell potential.

(continued on next page)

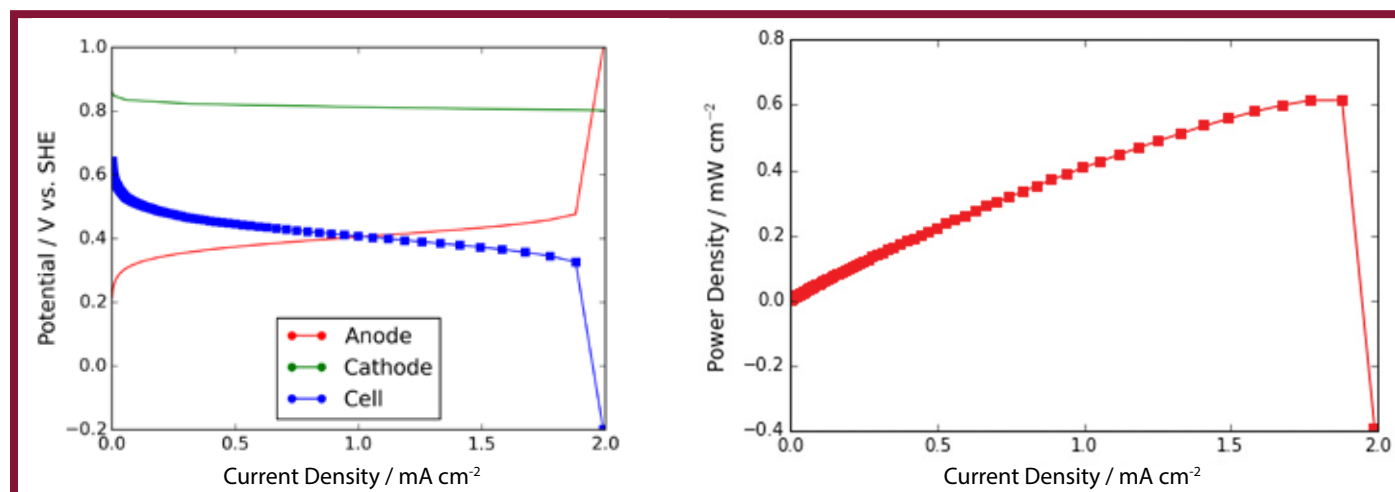


FIG. 3. Complete cell polarization by taking the difference between anode and cathode polarization curves. (a) Cell polarization. (b) Cell power density. Details of the calculation are available online.¹⁴

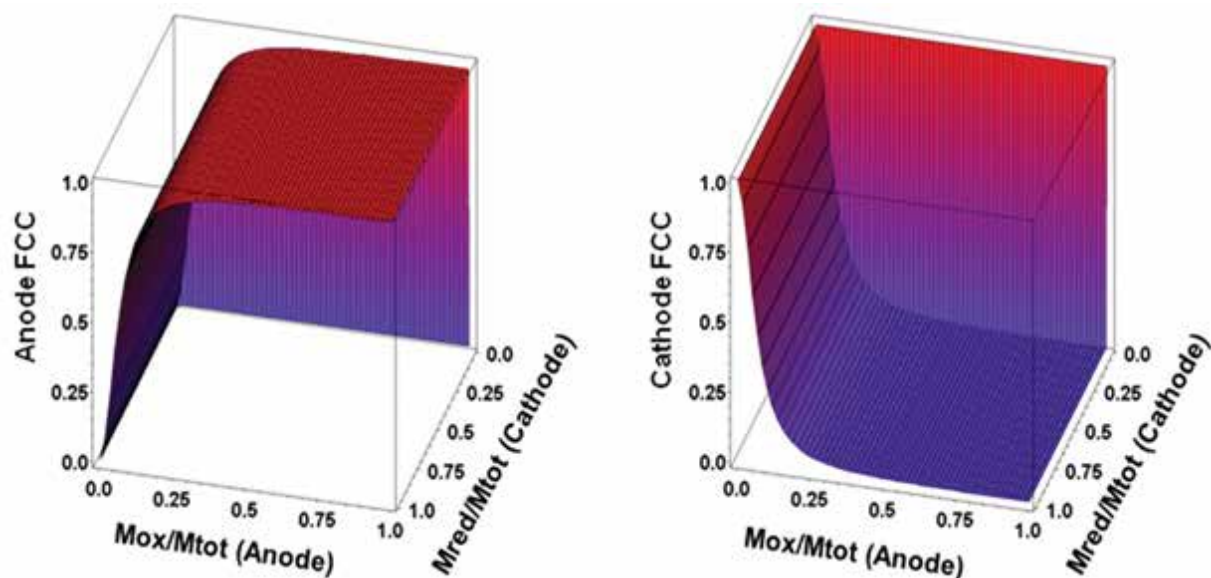


Fig. 4. Flux control coefficients (FCCs) for a mediated glucose anode (left) and oxygen cathode (right) as a function of mediator redox state (M_{ox}/M_{tot} for the anode and M_{red}/M_{tot} for the cathode) at ambient oxygen concentration (0.28 mM) and a total mediator concentration of 500 mM on each electrode.¹⁸

Assuming that transport limitations can be ignored and that enzyme kinetics control overall biofuel cell performance, metabolic control analysis (MCA) can be applied to determine the degree of control of each electrode reaction over the fuel cell performance. For example, Glykys et al. have constructed a detailed MCA model for the glucose-oxygen fuel cell, and considered the degree of control by each electrode in terms of a flux control coefficient (FCC).¹⁸ This model allowed a determination of the extent to which each electrode controlled cell current density and power at any potential, glucose concentration, or oxygen concentration (Fig. 4).

Parameterization

A challenging aspect of modeling bioelectrodes is determination of parameters. In particular, enzyme loadings and concentrations may be quite difficult to determine, and may change with time due to denaturation and de-immobilization. Often, nominal loading values are assumed, which do not account for these losses. In some cases, actual catalyst loadings may be determined analytically, for example using fluorescence approaches.^{19,20} This remains an ongoing challenge in this research area.

In the case of hydrogel bioelectrodes, the film thickness resulting from formation of the hydrogel introduces significant uncertainty. This thickness can be nonuniform and range from nanometer to millimeter scales. Film thicknesses have been determined using a variety of techniques, including confocal microscopy,²¹ profilometry,¹¹ and ellipsometry.²² Hydrogel film thickness is also dependent on the degree of hydration of the film, making ex-situ measurements challenging. The results of film thickness measurements have direct impact on estimates of enzyme, mediator concentrations as well as mediator effective diffusivity measurements.¹¹ Therefore, good estimates of these parameters are essential for determination of kinetic parameters from performance data using the present models.

Multi-Enzyme Cascades

The above models are simplistic for many reasons, one of which is the fact that only one enzyme is utilized in each electrode. Examples of multi-enzyme systems have been extensively reported recently, primarily for deep oxidation of complex fuels such as methanol, glucose, and ethylene glycol.²³⁻²⁵ Models of such systems have been reported, and include the enzyme kinetics for each individual step.^{26,27} For example, Osman et al. report a complete, transient model for a glucose-oxygen biological fuel cell utilizing both glucose dehydrogenase mediated diaphorase at the glucose anode (Fig. 5).²⁷ Kinetic parameters, primarily drawn from the literature, are sufficient to closely predict the performance of each half-cell and the resulting overall cell.

A significant challenge is to account for transport of intermediates between each reactant step, and to consider the reversibility of the enzyme kinetics. For sufficiently large polarization, this reversibility can be neglected because a key product (such as a reduced mediator or cofactor) may be assumed to be absent. At intermediate potentials, however, this assumption may not be appropriate and reversible rate expressions are required. Regarding intermediate transport, loss of intermediates from the electrode is a significant factor that must be accounted for in the model. This is particularly important because the turnover rates of adjacent reaction steps may vary widely.

Summary

The above discussion reflects a simplified approach to modelling of biological electrodes applicable to biological fuel cells, sensors, and bioreactors. These models are useful for describing the relationship between individual physical properties and overall electrochemical performance, and can be used for determination of unknown parameters and prediction of performance. Nonetheless, significant challenges arise in applying such models due to uncertainties in parameter estimation, and in the complex nonlinear kinetics and transport associated with enzymatic reactions. Such complexity increases with the number of biocatalysts included in a given electrode, and hence biological electrode modeling remains an area of significant research interest, with immense potential for further advances. ■

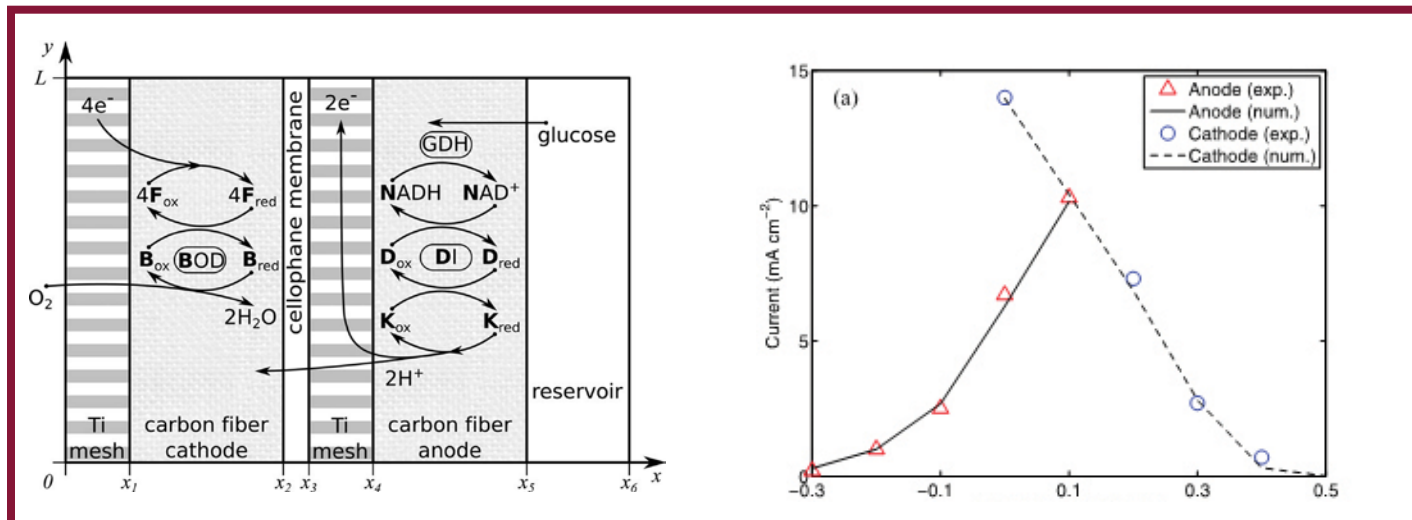


FIG. 5. Complete model of a Glucose-oxygen fuel cell utilizing glucose dehydrogenase and diaphorase at the anode.²⁷ (a) Model schematic. (b) Model results for each half-cell closely match experiment.

About the Author



SCOTT CALABRESE BARTON is an Associate Professor of Chemical Engineering at Michigan State University, where his research focuses on engineering and materials issues in low-temperature fuel cells, particularly transport processes in porous electrodes. His doctoral work in direct methanol fuel cells and zinc-air batteries at Columbia University led to postdoctoral studies of novel biofuel cell electrodes at the University of Texas at Austin. He is the recipient of a

CAREER award from the National Science Foundation and a Petroleum Research Fund award from the American Chemical Society. He currently serves as Chair of the Energy Technology Division of ECS. He may be reached at scb@msu.edu.

<http://orcid.org/0000-0002-1407-0275>

References

- H. R. Luckarift, P. B. Atanasso, and G. R. Johnson, *Enzymatic Fuel Cells: From Fundamentals to Applications*, Wiley, (2014).
- A. Illanes, *Enzyme Biocatalysis: Principles and Applications*, Springer Science, (2008).
- G. Binyamin, J. Cole, and A. Heller, *J. Electrochem. Soc.*, **147**, 2780–2783 (2000).
- M. Minson et al., *J. Electrochem. Soc.*, **159**, G166–G170 (2012). doi:10.1149/2.062212jes.
- S. Calabrese Barton, in *Handbook of Fuel Cells – Fundamentals, Technology and Applications*, W. Vielstich, H. A. Gasteiger, and H. Yokokawa, Editors, vol. 5, p. 112–130, John Wiley and Sons, Ltd., London (2009).
- M. Majda, in *Molecular Design of Electrode Surfaces*, R. W. Murray, Editor, vol. 22, p. 159–206, Wiley, New York (1992).
- J. M. Saveant, *J. Electroanal. Chem.*, **242**, 1–21 (1988).
- P. A. Frey and A. D. Hegeman, *Enzymatic Reaction Mechanisms*, Oxford University Press, (2007).
- H. M. Sauro, *Enzyme Kinetics for Systems Biology*, Ambrosius Publishing, (2012).
- P. N. Bartlett and K. F. E. Pratt, *J. Electroanal. Chem.*, **397**, 61–78 (1995). doi:10.1016/0022-0728(95)04236-7.
- J. W. Gallaway et al., *J. Am. Chem. Soc.*, **130**, 8527–36 (2008). doi:10.1021/ja0781543.
- T. Tamaki, T. Ito, and T. Yamaguchi, *Fuel Cells*, 37–43 (2009). doi:10.1002/fuce.200800028.
- L. Rajendran and K. Saravanakumar, *Electrochim. Acta*, **147**, 678–687 (2014). doi:10.1016/j.electacta.2014.08.126.
- S. Calabrese Barton, *Numerical model of a mediated Glucose Oxidase electrode*, <http://bit.ly/1GKKQlb>.
- T. Tamaki, T. Sugiyama, M. Mizoe, Y. Oshiba, and T. Yamaguchi, *J. Electrochem. Soc.*, **161**, H3095–H3099 (2014). doi:10.1149/2.0181413jes.
- S. C. Barton, Y. H. Sun, B. Chandra, S. White, and J. Hone, *Electrochem. Solid-State Lett.*, **10**, B96–B100 (2007). doi:10.1149/1.2712049.
- S. C. Barton, *Electrochim. Acta*, **50**, 2145–2153 (2005). doi:10.1016/j.electacta.2004.09.022.
- D. J. Glykys and S. Banta, *Biotechnol. Bioeng.*, **102**, 1624–1635 (2009). doi:10.1002/bit.22199.
- G. L. Martin, S. D. Minteer, and M. J. Cooney, *ACS Appl. Mater. Interfaces*, **1**, 367–372 (2009). doi:10.1021/am8000778.
- G. L. Martin, C. Lau, S. D. Minteer, and M. J. Cooney, *Analyst*, **135**, 1131–1137 (2010). doi:10.1039/b921409g.
- D. Chakraborty, S. Calabrese Barton, and S. C. Barton, *J. Electrochem. Soc.*, **158**, B440 (2011). doi:10.1149/1.3552592.
- D. Chakraborty, E. McClellan, R. Hasselbeck, and S. C. Barton, *J. Electrochem. Soc.*, **161**, H3076–H3082 (2014). doi:10.1149/2.0121413jes.
- Y. H. Kim, E. Campbell, J. Yu, S. D. Minteer, and S. Banta, *Angew. Chem. Int. Ed. Engl.*, **52**, 1437–1440 (2012). doi:10.1002/anie.201207423.
- D. P. Hickey, F. Giroud, D. W. Schmidtke, D. T. Glatzhofer, and S. D. Minteer, *ACS Catal.*, **3**, 2729–2737 (2013). doi:10.1021/cs4003832.
- D. Sokic-Lazic, R. L. Arechederra, B. L. Treu, and S. D. Minteer, *Electroanalysis*, **22**, 757–764 (2010). doi:10.1002/elan.200980010.
- P. Kar, H. Wen, H. Li, S. D. Minteer, and S. Calabrese Barton, *J. Electrochem. Soc.*, **158**, B580 (2011). doi:10.1149/1.3561690.
- M. H. Osman, A. A. Shah, and R. G. A. Wills, *J. Electrochem. Soc.*, **160**, F806–F814 (2013). doi:10.1149/1.059308jes.